

The Tologoi Key Section (Upper Cenozoic, Transbaikalia): Reconstruction of the Peculiarities and Depositional Environment

V.V. Ivanova^{a,d,h,✉}, M.A. Erbaeva^b, A.A. Shchetnikov^{c,d,e,f}, A.Yu. Kazansky^{g,h}, G.G. Matasova^{h,i},
N.V. Alekseeva^b, I.A. Filinov^{c,f,h}, M.I. Kuzmin^d

^aI.S. Gramberg All-Russia Scientific Research Institute for Geology and Mineral Resources of the Ocean (FSBI “VNIIOkeangeologia”),
Angliiskii pr. 1, St. Petersburg, 190121, Russia

^bGeological Institute, Siberian Branch of the Russian Academy of Sciences, ul. Sakh'yanovoi 61, Ulan-Ude, 670047, Russia

^cInstitute of the Earth's Crust, Siberian Branch of the Russian Academy of Sciences, ul. Lermontova 128, Irkutsk, 664033, Russia

^dVinogradov Institute of Geochemistry, ul. Favorskogo 1a, Irkutsk, 664033, Russia

^eIrkutsk Scientific Center, Siberian Branch of the Russian Academy of Sciences, ul. Lermontova 134, Irkutsk, 664033, Russia

^fIrkutsk State University, ul. Karla Marksa 1, Irkutsk, 664003, Russia

^gLomonosov Moscow State University, Leninskie Gory 1, Moscow, 119991, Russia

^hGeological Institute, Russian Academy of Sciences, Pyzhevskii per. 7, Moscow, 119017, Russia

ⁱTrofimuk Institute of Petroleum Geology and Geophysics, Siberian Branch of the Russian Academy of Sciences,
pr. Akademika Koptyuga 3, Novosibirsk, 630090, Russia

Received 10 October 2018; received in revised form 26 January 2020; accepted 27 March 2020

Abstract—This paper presents new data on the structure and lithologic, geochemical, and granulometric features of the Quaternary deposits of the Tologoi key section (upper Cenozoic, Transbaikalia). These data made it possible to determine the location of paleosol horizons throughout the section and their thicknesses. Four main sedimentation cycles have been identified; each of them terminated with the formation of soil horizons. It is shown that the climate during the formation of the deposits had a cyclic nature: Wet periods were changed by dry epochs of different durations. During warming and the formation of soil horizons, distant and medium-range provenance areas prevailed. *In situ* biochemical postsedimentary transformations of the deposits dominated in the periods of the most intense pedogenesis, as reflected in the changes in their chemical composition. It is shown that the warmest climate and the activation of weathering and leaching processes during the Pleistocene were in the period of the accumulation of a paleosol horizon in the section interval 16.4–15.0 m. It was a period of pedogenic and biologic activity and reduced salinization and carbonation. Stages with prevailing cryogenic environments are clearly recorded in the studied geochemical profile as involutions, pseudomorphs after ice wedges, and thick carbonate lenses. The deposits formed at these stages are characterized by minimum salinization, high calcification, and low leaching (hydrolysis) and oxidation indices as well as a positive Eu anomaly and high $\Sigma\text{Ce}/\Sigma\text{Y}$ and low La/Sm values.

Keywords: Pleistocene; Pliocene; geochemical composition of loose deposits; environmental changes; lithology; Tologoi key section; Transbaikalia

INTRODUCTION

The key section near Mt. Tologoi (Fig. 1A), discovered by A.P. Okladnikov in 1951, is located in the Ivolga depression on the left bank of the Selenga River, southwest of Ulan-Ude.

The section comprises a sequence of continental deposits of a wide age range: from the beginning of the late Pliocene

to the Holocene, with an insignificant sedimentation break (at the beginning of the Late Pleistocene). The first information about the section and its fauna was provided by Bibikova et al. (1953).

The section of Pliocene–Quaternary deposits near Mt. Tologoi was described by Aleksandrova et al. (1963) and Ravskii et al. (1964), and their chemical composition was studied by Liskun and Rengarten (1963). Based on these data, the authors drew conclusions about the genesis of the deposits and divided the section into two parts: The lower-section red-colored deposits are products of the proximal

✉ Corresponding author.

E-mail address: Vargeo66@gmail.com (V.V. Ivanova)

redeposition of red-colored weathering crust in a shallow lake, and middle- and upper-section pale gray sandy and sandy-loam deposits are of deluvial–proluvial origin. As established earlier (Ravskii et al., 1964; Vangengeim et al., 1966; Ivan'ev, 1966; Bazarov, 1986; Erbaeva, 1970; Vangengeim, 1977), the multilayered section of loose deposits near Mt. Tologoi is a key section not only for western Transbaikalia but also for East Siberia as a whole. It is unique by the presence of the continental deposits of the Ivolga depression, which accumulated with short temporal breaks from the end of the middle Pliocene through the Holocene.

The three units identified in the section are three stratigraphic levels (Alekseeva, 2005) (Fig. 1B): upper (Holocene, Upper Pleistocene), middle (Middle–Lower Pleistocene), and lower (upper Pliocene). The section basement contains red-colored deposits, which are considered to be the stratotype of the Chikoi (Tologoi) Formation (Bazarov, 1968). In the upper part of the middle unit of the Tologoi section, the Brunhes–Matuyama reversal boundary was established (Gnibidenko et al., 1976). A specific feature of the deposits is the presence of paleosol horizons in the three units (Ravskii et al., 1964; Vangengeim et al., 1966; Bazarov, 1968; Erbaeva, 1970; Alekseeva, 2005). The rocks located beneath the Brunhes–Matuyama reversal show signs of a cryogenic impact (Alekseeva, 1994; Vogt et al., 1995; Alexeeva and Erbaeva, 2000) indicating that the first permafrost appeared in western Transbaikalia at least at the end of the Early Pleistocene rather than the Late Pleistocene, as believed earlier (Bazarov, 1968; Ravskii, 1972).

In 1993, detailed paleontological studies were carried out in the Mt. Tologoi exposure, at five step strippings (parallel to the main one) of the upper and middle units (Alekseeva, 2005). Relics of small mammals were collected from 13 horizons (earlier, from six horizons only); their composition gave an insight into the successive evolution of biota from Pliocene to Holocene. Later, during these strippings, Ryashchenko et al. (2012) thoroughly documented and sampled loess-like deposits, paleosols, and Pliocene red clays and obtained information about the microstructural parameters and the content of clay minerals in them.

In the middle unit of the Tologoi section, the first (lower, ~1 Ma) and second (middle, ~800 ka) paleosol horizons were described and sampled. The horizons have common features, such as the pale gray color, rock aggregation, macroporosity (there are different types of macropores), and presence of carbonates (Ryashchenko et al., 2012). According to the authors, the aggregation and macroporosity are the result of periodically repeated degradation of permafrost, which had formed during eight cooling cycles since the early Pleistocene. The formation of paleosol horizons in the loess unit was due to climate warming. The prevailing chestnut soils formed in a dry-steppe zone with unsteady humidification. The paleosols are almost indistinguishable from loess-like deposits in geologic, lithologic, and microstructural features. The Pliocene clays, a regional substrate of loess units, are characterized by the reddish-brown color, a

lumpy/platy structure, and cemented gruss and gravel and also show loess features, such as powderiness, macroporosity, and presence of carbonates. It is likely that the clays acquired these features under cryogenic impacts in the Pleistocene cooling periods.

Recent investigations have provided new information about the formation and structure of Holocene and Late Pleistocene paleosols as well as the first absolute dates for sediments and paleosols (Andreeva et al., 2011; Zech et al., 2017).

In this work we present results of a multidisciplinary study of the Tologoi section deposits by granulometric and lithochemical methods and approaches. The goal of the study was to clarify the lithologic and stratigraphic structure of the section and to reconstruct the paleoecologic conditions of its formation. We have first described the geochemical composition of the section deposits and confirmed the informative value of REE patterns and some petrochemical indices for refining the formation conditions of the Quaternary deposits. We also show the applicability of REE fractionation coefficients to paleoecological reconstructions.

MATERIALS AND METHODS

Our research was based on a comprehensive analysis of the lithology of the loose deposits of the Tologoi section with the use of grain size and geochemical data. In this work we apply geochronological terms following the International Chronostratigraphic Chart, according to which the Pliocene–Pleistocene boundary is dated at 2.588 Ma.

To examine the grain size composition of the Tologoi deposits, samples have been collected at 10 cm spacing in the complete profile of the section. The studied collection comprised 222 samples.

Granulometric studies were carried out on a Microtrac X100 laser particle size analyzer. The sizes of the particles under study ranged from 704 to 0.146 μm . For convenience, the particles were combined into 50 fractions, whose contents (vol.%) were determined for each sample. The samples were dispersed by ultrasonic treatment.

The results obtained for all samples were processed using the statistical GRADISTAT software (Blott and Pye, 2001). For each sample, we determined the distribution modes and calculated the median and average grain sizes, grading, asymmetry, and eccentricity. For a statistical analysis, the measured samples were separated into four fractions according to the sizes of rock particles and fragments: sand (>100 μm), coarse silt (50–100 μm), fine silt (10–50 μm), and clay (<10 μm) (classification after Raukas (1981)). The clay fraction includes a silt subfraction (<2 μm). The calculations were made by the method of arithmetic moments (Gradziński et al., 1976) and by the Folk–Ward (1957) method modified by Blott and Pye (2001), which yields more accurate estimates for the grain size description of the samples. In addition, we used the following calculated pa-

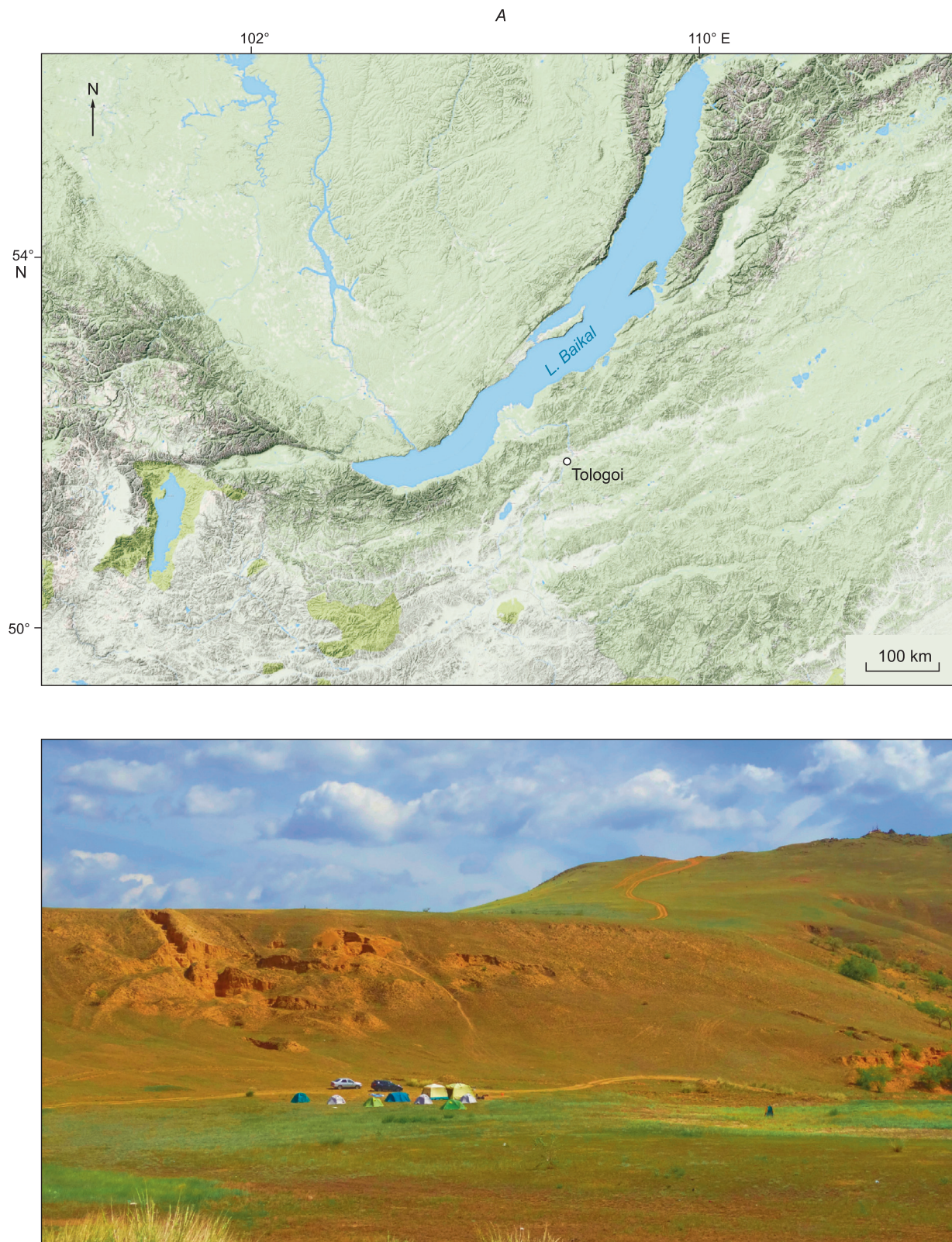
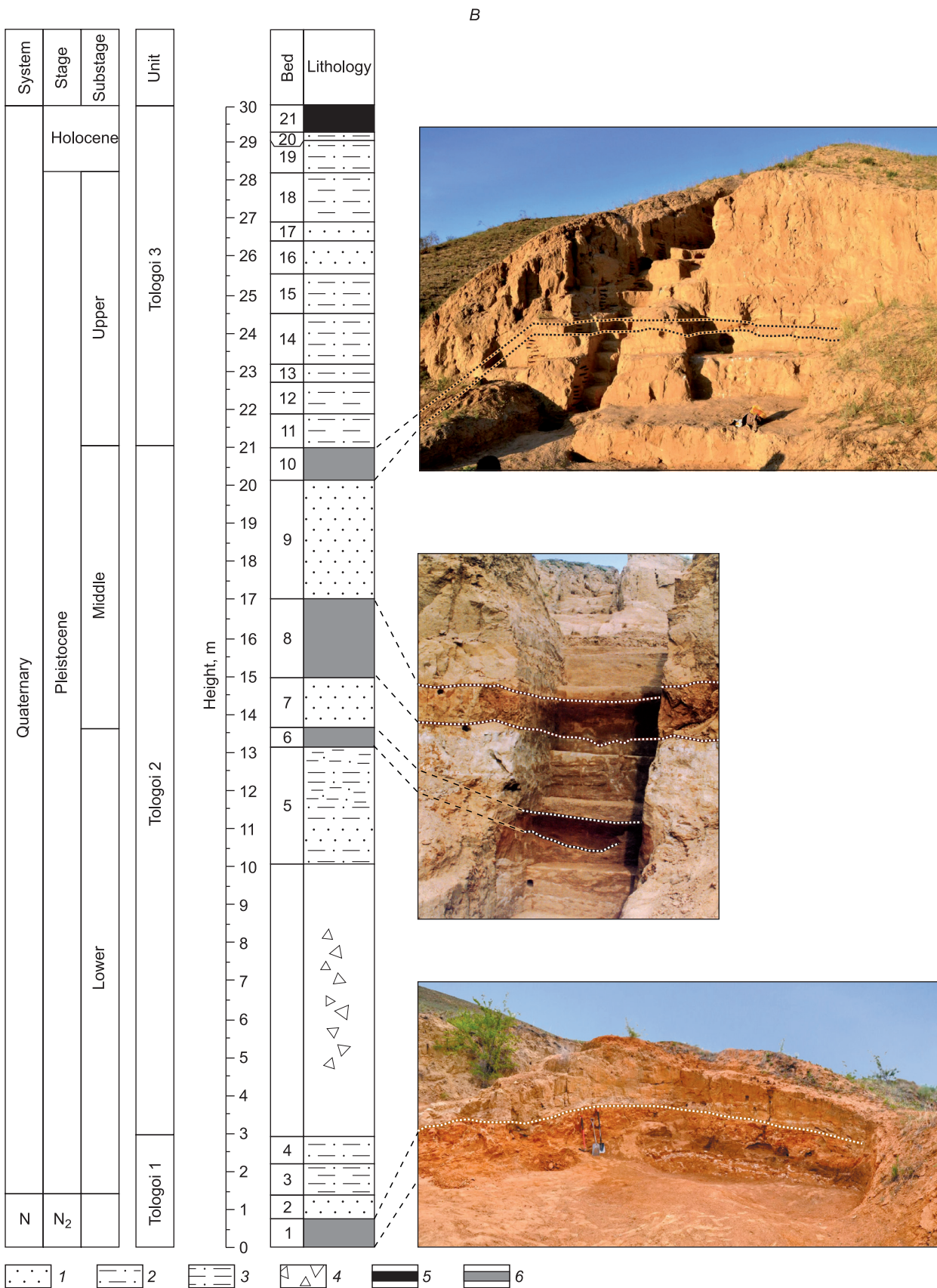


Fig. 1. General map of the study area with the location of the Tologoi key section (A). Stratigraphy and lithology of the Tologoi section and its photographs (by I.A. Filinov and M.A. Erbaeva) showing the position of paleosols (B). 1, sands, 2, sandy loams, 3, loams, 4, talus, 5, recent soil, 6, paleosol.



rameters: D_{av} , the average grain size, calculated as a weighted average (Gradziński et al., 1976); F , a dynamic factor, the ratio of the amount of physical sand (the total content of the $>50 \mu\text{m}$ fractions) to the amount of physical clay (the total content of the $<50 \mu\text{m}$ fractions) in the sample. This parameter marks the sedimentation conditions: At $F > 1$, clastic material is supplied mostly from proximal and medium-range (up to ten kilometers) sources through dragging and saltation, which is, most likely, the case in a highly dynamic medium with strong eddy winds. At $F < 1$, the supply of clastic material is reduced, and substance arrives in the form of air aerosols, mainly from distant sources; *in situ* postsedimentary transformations of the deposits (mainly soil-forming ones) prevail (Kazansky et al., 2018); k , dispersion index reflecting the type of clay components and the degrees of their “washing”, “leaching”, and “illuviation”; it marks podsolization, claying, etc. associated with the transformation, transfer, and localization of finely dispersed substance in various deposits. The index is calculated by the formula (Berezin, 1983):

$$k = (\ln F5 - \ln F1) / 1.609,$$

where $F5$ is the content of particles with a diameter of $<5 \mu\text{m}$ (%) and $F1$ is the content of particles with a diameter of $<1 \mu\text{m}$ (%).

The chemical composition of the Tologoi section deposits was established by petrochemical studies of terrigenous rocks (222 samples, 0.1 m sampling interval). The contents of trace and dispersed elements (Li, Ba, Sc, Cu, Zn, Co, Ni, Y, Nb, Cs, Th, and U) in the rocks were determined by X-ray fluorescence spectroscopy (Institute of the Earth's Crust, “Geodynamics and Geochronology” Common Use Center, Irkutsk), and the contents of rock-forming oxides, by the wet chemistry method. The oxide contents were recalculated to the calcined carbonate-free sample and then to the molar mass for the calculation of the main petrochemical parameters.

The contents of REE in the particular samples (22 samples, 0.9 m sampling interval) were measured by ICP MS (Institute of Geochemistry, Irkutsk) with a relative error of 5–10%.

Statistical processing of the analytical results was made using the Statistica 10.0 software.

For the general description of the Tologoi section deposits, we analyzed the distribution of some geochemical parameters (loss on ignition (LOI), Cr contents, and Co/Zr and Cu/Zr ratios) and major lithochemical indicators of the paleoclimate (petrochemical indices: HI, hydrolysate, FI, femic, TM, titanium, SI, sodium, PI, potassium, AI, alkali, NAI, normalized alkalinity, ASI, aluminosilicic) (Yudovich and Ketris, 2000; Maslov, 2005)¹.

¹HI = $(\text{Al}_2\text{O}_3 + \text{TiO}_2 + \text{Fe}_2\text{O}_3 + \text{FeO} + \text{MnO})/\text{SiO}_2$; FI = $(\text{Fe}_2\text{O}_3 + \text{FeO} + \text{MnO} + \text{MgO})/\text{SiO}_2$;

TI = $\text{TiO}_2/\text{Al}_2\text{O}_3$; SI = $\text{Na}_2\text{O}/\text{Al}_2\text{O}_3$; PI = $\text{K}_2\text{O}/\text{Al}_2\text{O}_3$; AI = $\text{Na}_2\text{O}/\text{K}_2\text{O}$; NAI = $(\text{Na}_2\text{O} + \text{K}_2\text{O})/\text{Al}_2\text{O}_3$; ASI = $\text{Al}_2\text{O}_3/\text{SiO}_2$.

The qualitative and quantitative nature of the geochemical signal as applied to young loose continental deposits and their comparative characteristics are described in the summary research works (Maslov, 2005, 2006).

To estimate the intensity of sedimentation and pedogenesis, we used the following parameters:

– chemical index of alteration, CIA = $(\text{Al}_2\text{O}_3/(\text{Al}_2\text{O}_3 + \text{CaO} + \text{Na}_2\text{O} + \text{K}_2\text{O})) \cdot 100$ (Nesbitt and Young, 1982);

– chemical index of weathering, CIW = $(\text{Al}_2\text{O}_3/(\text{Al}_2\text{O}_3 + \text{CaO} + \text{Na}_2\text{O})) \cdot 100$ (Fedo et al., 1995);

– index of compositional variability, ICV = $(\text{Fe}_2\text{O}_3 + \text{K}_2\text{O} + \text{Na}_2\text{O} + \text{CaO} + \text{MgO} + \text{TiO}_2)/\text{Al}_2\text{O}_3$ (Cox et al., 1995);

– plagioclase index of alteration, PIA = $((\text{Al}_2\text{O}_3 - \text{K}_2\text{O})/(\text{Al}_2\text{O}_3 + \text{CaO} + \text{Na}_2\text{O} - \text{K}_2\text{O})) \cdot 100$ (Fedo et al., 1995);

– hydrolysis intensity index $\text{Al}_2\text{O}_3/(\text{CaO} + \text{Na}_2\text{O} + \text{K}_2\text{O} + \text{MgO})$ marking the ratio of clay component Al_2O_3 to major cations removed from soil into soil solutions (Retallack, 2001);

– calcification index $(\text{CaO} + \text{MgO})/\text{Al}_2\text{O}_3$ marking the accumulation of calcite and dolomite in soils (Retallack, 2007);

– Ba/Sr ratio characterizing the hydrothermal conditions of sedimentation, in particular, leaching (Retallack, 2001); Ba is part of K-feldspar and is less removed from soils than Sr associated with carbonates;

– oxidation index $(\text{Fe}_2\text{O}_3 + \text{MnO})/\text{Al}_2\text{O}_3$ (Kalinin et al., 2009).

The paleoecologic conditions of the section formation were described in detail using the following specific geochemical markers (Balashov, 1976; Elderfield and Greaves, 1982; Taylor and McLennan, 1985; Trueman et al., 2006; Shatrov, 2007; Ivanova, 2012; Ivanova et al., 2016):

(1) $\sum(\text{REE} + \text{Y})$, the total content of REE and Y, depending on both the composition of rocks subjected to washout and the fractionation of lanthanides in the hypergenesis zone. In addition, the total contents of LREE ($\sum\text{LREE} = \text{La} - \text{Pr} - \text{Nd}$), MREE ($\sum\text{MREE} = \text{Sm}, \text{Eu}, \text{Gd}, \text{Tb}, \text{Dy}, \text{and Ho}$), and HREE ($\sum\text{HREE} = \text{Er}, \text{Tm}, \text{Yb}, \text{and Lu}$) were evaluated.

(2) $\sum\text{Ce}/\sum\text{Y}$ ($\sum\text{Ce} = \text{La} - \text{Eu}$ and $\sum\text{Y} = \text{Gd} - \text{Lu}$ and Y), the index marking the intensity of weathering on land, where feldspars and accessory Ce-minerals disintegrate more intensely under humid lithogenesis, which results in a $\sum\text{Ce}/\sum\text{Y}$ increase. Our earlier study (Ivanova et al., 2017) showed that this index increases under cryogenic conditions because of the enrichment of the fine fraction of deposits with feldspars and hydromicas and of the transformation of the hydromicas as a result of cryogenic weathering.

(3) The cerium anomaly, expressed as $\text{Ce}^* = 3\text{Ce}_n/(2\text{La}_n + \text{Nd}_n)$ (Taylor and McLennan, 1985), is an indicator of the redox conditions of sedimentation (the NASC-normalized (Gromet et al., 1984) REE contents are considered).

(4) The europium anomaly, expressed as $\text{Eu}^* = 2\text{Eu}_n/(\text{Sm}_n + \text{Gd}_n)$ (Balashov, 1976), is an indicator of the supply of deep-seated material into sediments (the NASC-normalized (Gromet et al., 1984) REE contents are considered). The average Eu^* value for Phanerozoic deposits is 0.61–

0.72 (Balashov, 1976), and that for post-Archean sedimentary rocks is 0.65 (Taylor and McLennan, 1985).

(5) The La/Yb and La/Sm ratios are indicators of the physicochemical (pH, Eh) and facies conditions of diagenesis (Reynard et al., 1999; Trueman et al., 2006; Shatrov, 2007; Ivanova et al., 2017) (the NASC-normalized (Gromet et al., 1984) REE contents are considered).

(6) The LREE/HREE ratio, calculated as $[(La + Pr + Nd)/(Er + Tm + Yb + Lu)]_{sample} / [(La + Pr + Nd)/(Er + Tm + Yb + Lu)]_{NASC}$ (Maslov et al., 2007), is an indicator of volcaniclastic rocks, marks the proportion of felsic and mafic rocks in provenance areas, and characterizes the degree of carbonation: Light lanthanides isomorphically substitute Ca in the lattice of carbonate minerals (Kučera et al., 2009).

The statistical validity of the tetrad effect (Monecke et al., 2002) of REE of the third (Nd, Sm, Eu, and Gd) and fourth (Er, Tm, Yb, and Lu) tetrads is an indicator of the degree of MREE and HREE fractionation (Ivanova, 2012; Ivanova et al., 2016), calculated by the formula

$$T_i = \sqrt{\frac{1}{2} \cdot \left(\left(\left(\frac{v_2}{\sqrt[3]{v_1^2 \cdot v_4}} \right) - 1 \right)^2 + \left(\frac{v_3}{\sqrt[3]{v_1 \cdot v_4^2}} - 1 \right)^2 \right)}$$

where $i = 3, 4$ and v_1-v_4 are the NASC-normalized REE contents in the corresponding tetrad.

The type of tetrad effect, t (Irber, 1999) is calculated as

$$t_i = \sqrt{\frac{v_1 \cdot v_4}{v_2 \cdot v_3}}$$

The tetrad effect is considered statistically valid when t_i is greater than 0.2. The $t < 0.8$ values mark the W -type tetrad effect, and the $t > 1.1$ values indicate the M -type tetrad effect.

The statistical validity and the type of tetrad effect can be regarded as indicators of the physicochemical conditions of sedimentation and diagenesis.

THE LITHOLOGY AND STRATIGRAPHY OF THE TOLOGOI SECTION

The section near Mt. Tologoi is located in the Ivolga depression on the left bank of the Selenga River, southwest of Ulan-Ude. Tologoi is a residual pedimented granite pluton separated from the Ganzurin Ridge by the incised meander of the Selenga River. In the scarp of the incised meander, a complex of Pliocene–Quaternary deposits leant against the Tologoi base is revealed (Fig. 1B).

The section of loose deposits is clearly divided into three units of different ages (Tologoi 1–Tologoi 3) according to the detailed biostratigraphic characteristics reported by Alekseeva (2005). Each unit rests erosively upon the underlying rocks; moreover, the middle unit is separated from the upper one by a paleosol horizon.

The section structure is as follows (from bottom to top):

The lower unit (Tologoi 1)

The Upper Pliocene

Thickness, m

Layer 1. Highly compact cherry to dark brown loam with a sand and gravel impurity. Paleosol	0.7
Layer 2. Red to dark chocolate clayey sand. At the base, a carbonate nodule horizon up to 15 cm thick is traceable. The boundary with the underlying layer is well-defined, low-angle wavy. Slope deposits	0.6

The lower part of the Lower Pleistocene

Layer 3. Pink compact platy sandy loam with intercalates of pale yellow dust sand and whitish thin-laminated carbonated sandy loam. The boundary is clear, low-angle wavy. Loessivated slope deposits	0.8
Layer 4. Poorly sorted and poorly laminated pale yellow massive sandy loam with a gravel impurity. The boundary is poorly defined and gradient. Deluvium	0.7
Talus	4–7

The middle unit (Tologoi 2)

The upper part of the Lower Pleistocene

Layer 5. Poorly laminated pale yellow sandy loam with lenses and intercalates of poorly sorted gravel Sand and with lenses of whitish carbonated sandy loam. Numerous carbonate concretions. The boundary is clear, low-angle wavy. Deluvium.....	3
Layer 6. Reddish-brown sandy loam. The boundary is clear, low-angle wavy. Paleosol	0.6

The Middle Pleistocene

Layer 7. Poorly sorted, poorly laminated pale yellow dusty sand–gravel deposits with lenses of oblique coarse-grained sand and intercalates of whitish carbonated sandy loam. The boundary is clear, low-angle wavy. Proluvial–deluvial deposits	1.3
Layer 8. Reddish-brown sandy loam. The boundary is clear, low-angle wavy. Paleosol	2.3
Layer 9. Poorly sorted fine-grained pale yellow dusty sand with lenses of gravel sand. The bedding is poorly defined low-angle wavy and lenticular. The boundary is clear and smooth. Deluvium	2.8
Layer 10. Brown massive sandy loam with a platy structure. The boundary is clear, low-angle wavy. Paleosol	1

The upper unit (Tologoi 3)

The Upper Pleistocene

Layer 11. Pale brownish-yellow, whitish porous sandy loam. The deposits are highly carbonated. The boundary is unclear, low-angle wavy. Loess-like deposits	1.7
---	-----

Layer 12. Pale brownish-yellow, whitish porous sandy loam with gravel lenses, interbedded with sandy loam and sand. The deposits are highly carbonated. The boundary is unclear, low-angle wavy. Loessivated deluvium	0.5
Layer 13. Poorly sorted, poorly laminated pale yellow sandy loam with coarse-grained sand and gravel. Deluvial–proluvial deposits. The boundary is unclear, low-angle wavy	1.4
Layer 14. Pale yellow sandy loam with lenses and intercalates of gravel and whitish porous carbonated sandy loam. The bedding is wavy and lenticular. The bottom of the layer is strongly cryoturbated, with involutions from the underlying deposits. Loessivated deluvium	1.3
Layer 15. Pale yellow sandy loam with sand and gravel, interbedded with whitish, highly carbonated sandy loam. The bedding is thin wavy parallel. The boundary is clear wavy. Loessivated deluvium	0.3
Layer 16. Pale yellow inequigranular sand with gravel intercalates, interbedded with whitish, highly carbonated sandy loam. The bedding is thin, low-angle wavy. The boundary is unclear. Loessivated deluvium	0.6
Layer 17. Pale yellow carbonated sandy loam with thin intercalates of coarse-grained sand. The boundary is clear wavy. Loessivated deluvium	0.6
Layer 18. Interbedded pale yellow, whitish (due to carbonation) sandy loams and coarse-grained and gravel sand. The bedding is low-angle wavy, rhythmic; the interbeds are 3–5 cm thick. The boundary is well-defined wavy. Deluvium.....	0.8

Holocene

Layer 19. Poorly sorted pale yellow, whitish (due to carbonation) massive sandy loam. The boundary is sharp and wavy. Loessivated slope deposits	0.9
Layer 20. Pale sandy loam with gravel lenses. Loessivated slope deposits	0.2
Layer 21. Dark gray homogeneous massive sandy loam. The boundary is gradient. Recent soil	0.7

THE GRAIN SIZE COMPOSITION OF DEPOSITS

The variations in all grain size parameters throughout the section are shown in Fig. 2.

Paleosols are identified as layers of light to medium-weight fine-grained loam. The dynamic factor F is the formal parameter for their identification. It characterizes the sedimentation conditions: At $F > 1$, clastic material is supplied mostly from proximal and medium-range (up to ~10 km) sources through dragging and saltation, which is most likely in a highly dynamic environment with strong gusty winds; at $F < 1$, the supply of clastic material diminishes, and air aerosols inflow, mainly from distant sources; in the latter conditions, *in situ* postsedimentary transformations of deposits (mainly pedogenesis (Kazansky et al., 2018)) prevail. The low values of the dispersion coefficient k indicate the presence of finely dispersed material.

Based on the grain size data, we have identified six paleosols in the section. The upper paleosol (layer 17, depth range 26.8–26.2 m) is poorly developed and is not visible in the deposits. Layer 6 (13.6–13.0 m) is a strongly denuded soil horizon but is clearly identified by color and texture. These soils are characterized by smaller average grain size (D_{av}) as compared with the host deposits (120–150 μm against 140–375 μm).

Two horizons of paleosols in the middle section (Tologoi 2, layers 10 and 8) are clearly pronounced, 1–2 m thick, with $D_{av} = 73\text{--}88 \mu\text{m}$.

The paleosol in the lower section (Tologoi 1) is clearly expressed, 0.7 m thick, with $D_{av} = 113\text{--}150 \mu\text{m}$ and $F < 1$. Its deposits are poorly sorted, which is apparently due to the specific genesis of the lower-unit deposits (products of the proximal redeposition of red-colored weathering crust in the shallow-lake environment). The substrate is enriched in fine detrital material, which is due to the proximity of the bed-rock shores.

Based on the grain size indices in the upper and middle sections, we have distinguished a few levels with coarsest-grained deposits: 28.0–27.0, 26.0–25.2, 23.0–21.0, and 18.7 m. Beginning from the level of 14.6 m, the average grain size monotonically increases throughout the section, except for the soil horizon.

The object of our discussion is layer 14 (the section interval 24.5–23.4 m, Tologoi 3, upper section) characterized by a high (relative to the other layers) content of clay fraction, a smaller average grain size, low k values, and $F < 1$. All these parameters are close to those of the soil horizons localized in the section intervals 21.0–20.0 and 16.4–15.0 m (layers 10 and 8, respectively) and are different from the parameters of the underlying and overlying deposits.

Since the deposits, except for the paleosols, contain 40–80% sand fraction (>100 μm) and 65–95% physical sand (the sum of coarse-silt and sand fractions), it makes sense to consider thoroughly the composition of the sand fraction, i.e., the contents of fine-grained (100–250 μm), medium-grained (250–500 μm), and coarse-grained (>500 μm) sand (Fig. 2, on the right).

In the assumed paleosol intervals, the deposits are composed predominantly of fine-grained sand and lack coarse-grained sand (the only exception is the uppermost (26.8–26.2 m) poorly developed soil). In general, the distribution of sand fractions in the intervals is the same and even clearer than in other layers.

As follows from the obtained data, the section is made up of cyclically alternating sands, sandy loams, and loams (Fig. 2). The cyclicity of sedimentation is best seen in the diagrams of sand fractions (Fig. 2, on the right). It is expressed as the reduced (or even no) supply of coarse-grained sand (formation of loess-like sandy loam) in certain periods and an increase in the amount of this sand fraction to 20–30% (and up to 70% in the section interval 26–25 m) in other periods (formation of coherent sands). There are four such cycles in the diagrams of the Tologoi 2 and Tologoi 3

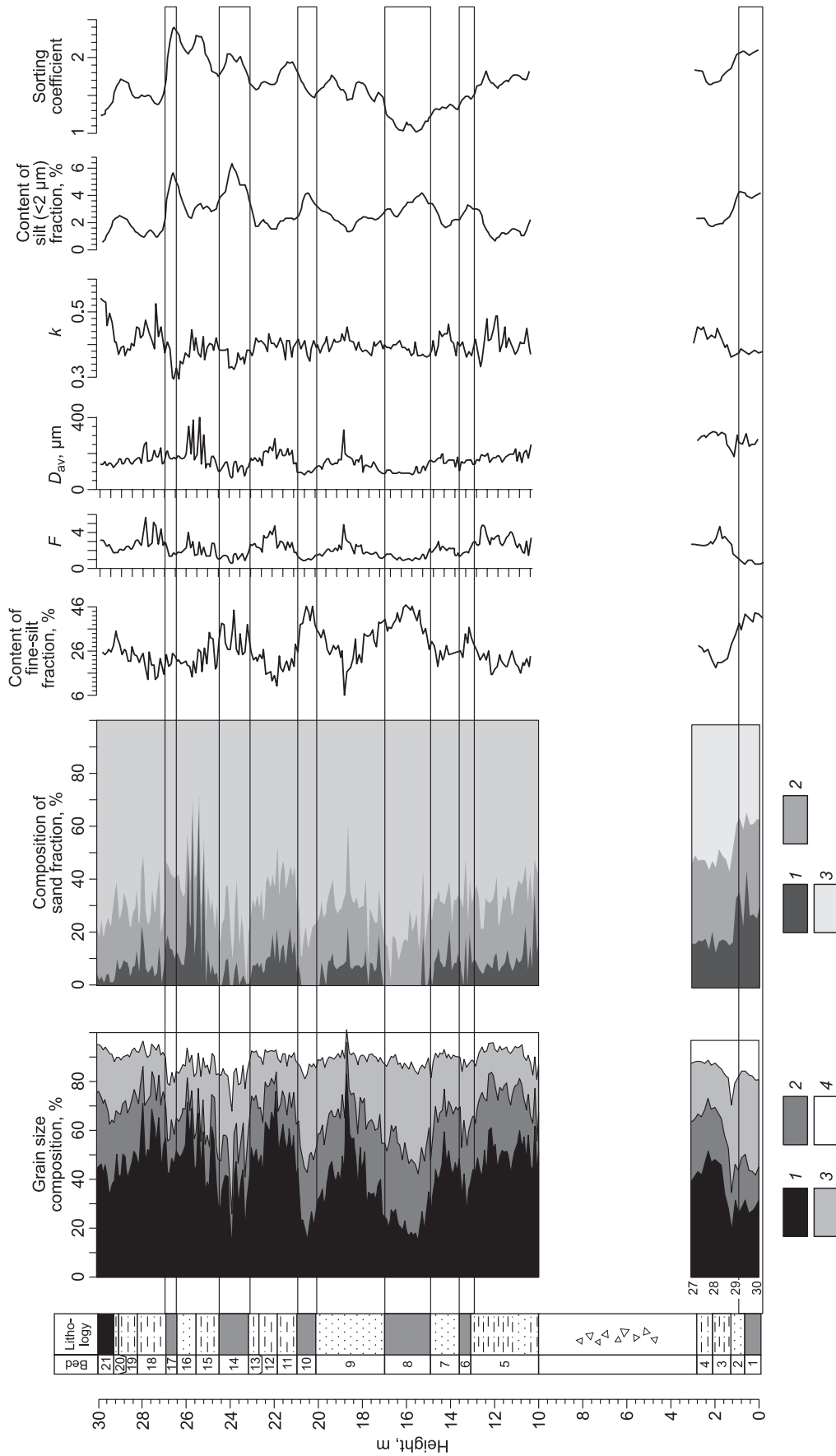


Fig. 2. Grain size composition of the Tolgoi section deposits. *F*, a dynamic factor, D_{av} , the average grain size, *k*, dispersion index. Lithologic composition, designations follow Fig. 1. Grain size composition: fractions: 1, sand, 2, coarse-silt, 4, fine-silt, 3, fine-silt, 2, medium-grained (>500 μm), 3, fine-grained (100–250 μm).

units; all of them terminated with the formation of soil horizons, including the recent soil. All soils in this part of the section (including the recent one) are more uniform in grain size and, accordingly, are better sorted than the sand and sandy loam deposits.

Based on the grain size parameters, the upper section can be divided into two units, Tologoi 2 and Tologoi 3, with the boundary between them running approximately along the paleosol of layer 10 (the section interval of 21–20 m). The upper unit, Tologoi 3, is composed of deposits with a widely varying grain size composition; most of them are moderately and insufficiently sorted (Fig. 2). The Tologoi 2 unit formed in the quiet-sedimentation regime with the gradually changing values of grain size parameters within the layers. Most of the deposits here are moderately sorted; in the section interval 17–13 m, they are even well sorted. Layers 7, 8, 9, and 10 formed as a single unit, without significant breaks in sedimentation. Short breaks were possible before and after the pedogenesis. The upper part of the Tologoi 2 unit (layers 11–21) completely formed in the regime of variable sedimentation or denudation; this is also evidenced by drastic jumps in parameters within the layers and at their boundary.

The average dispersion index (k) of the clayey deposits in the Tologoi section is equal to 0.4, which indicates their fine-dusty texture, weak pedogenesis processes, and a predominance of chlorite–illite group minerals among the clay minerals.

Thus, the grain size analysis of the deposits shows the following specifics of sedimentation in the Tologoi section:

(1) Cyclic sedimentation traced from the behavior of all fractions, especially from the change in sand content. Four main sedimentation cycles have been identified within the Tologoi 2 and Tologoi 3 units; each cycle terminated with the formation of soil horizons.

(2) Most of the deposits have a complex grain size composition. They are formed by populations of grains of different sizes, which are often present in equal or commensurate amounts, with sand grains being predominant. Sand fractions are usually supplied through dragging for short (few kilometers) distances. The second largest population is coarse-silt grains, which are transported mainly through saltation. Grains of this size might be supplied from a provenance area located few tens of kilometers from the sedimentation site. The third (fine-grained) population is a fine-silt fraction, which is transported with an air suspension. Such grains can be brought from distances of hundreds of kilometers. The fourth population is a clay or clay–silt fraction. The silt fraction has grains smaller than 2 μm (Fig. 2). Variations in its amounts reflect the influence of several processes. Its high content in paleosols is due to the postgenetic transformation of deposits during pedogenesis and cryogenesis and, thereby, to the formation of clay minerals (Dobrovolskii, 1976). The silt fraction in paleosols amounts to 4–7 vol.% and thus is a significant component of the deposits under study. During deluvial processes, fine-grained

material was removed through a sheet flood, which resulted in the reduced contents of silt fraction in the deluvial layers.

(3) Sedimentary material was transported to the sedimentation site mainly from a proximal source. In the periods of warming and the formation of soil horizons, wind gusts and strength were reduced; thereby, distant and medium-range provenance areas prevailed. In the periods of the most intense pedogenesis, the supply of sandy material decreased, sometimes to zero (Fig. 2), and *in situ* biochemical post-sedimentary transformations of deposits dominated.

(4) If the specific grain size parameters of the deposits were climate-controlled, then we assume that this area of the Selenga River valley had an arid climate with a minor humidity increase in the periods of pedogenesis. In dry periods, strong hurricane gusts and intense eolian processes were likely.

(5) The deposits of the Tologoi 2 unit (the section interval 20–10 m) formed in quieter wind conditions as compared with the Tologoi 3 unit.

(6) The regular change in the grain size parameters of the deposits reflects the specific sedimentation, pedogenesis with cryogenic transformation of the substrate, and deluvial redistribution of material along the slope. Taking into account the grain size composition, we interpret the genesis of the Tologoi 2 and Tologoi 3 deposits as deluvial (or eolian–deluvial and secondary deluvial).

GEOCHEMICAL COMPOSITION OF THE DEPOSITS

Major and trace elements. Analysis of the bulk chemical composition of the Tologoi section deposits shows minor variations in the contents of major oxides (except for CaO and CO₂) and trace elements (except for Cr).

The petrochemical indices demonstrate minor variations, which indicates intense mixing and homogenization of the deposits during the slope processes.

The high values of the alkali (AI) and normalized-alkalinity (NAI) indices and the low values of the hydrolysate index (HI) indicate a predominance of quartz and feldspar in the deposits and a low content of clay minerals. A significant amount of feldspars is also evidenced by the high NAI values (>0.4).

According to the average HI value (0.29), the studied rocks can be referred to as hypohydrolysates, i.e., rocks poorly transformed by weathering processes. The sodium index (SI) reflects the intensity of chemical weathering and the maturity of the supplied material. The higher the degree of chemical differentiation of material in the catchment paleoareas, the lower the SI (Akul'shina, 1990). The studied deposits are characterized by an extremely low degree of chemical differentiation; their SI value varies from 0.17 to 0.26 (for a weak chemical differentiation, SI is greater than 0.03). Comparison of the AI, SI, and PI values shows that the prevailing mineral of the section deposits is plagioclase rather than K-feldspar.

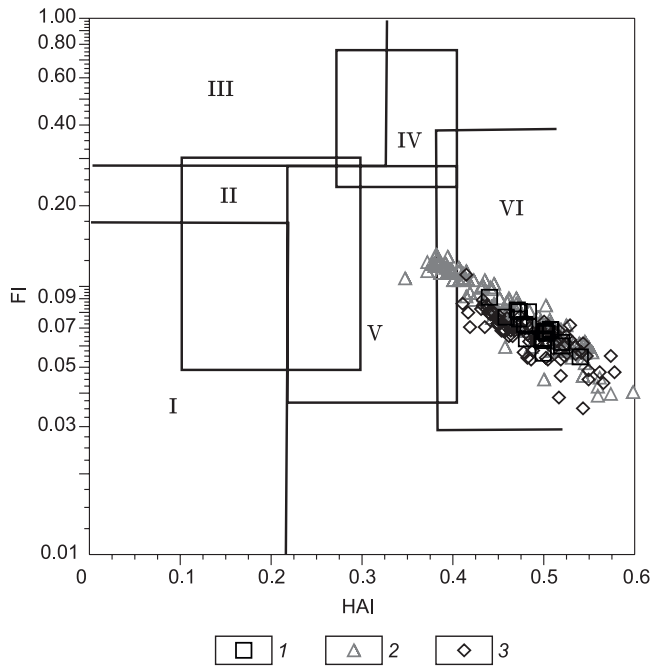


Fig. 3. FI-NAI diagram (Yudovich and Ketris, 2000). Units: I, Tologoi 1, 2, Tologoi 2, 3, Tologoi 3. I, mostly kaolinite rocks, II, mostly smectite rocks with kaolinite and hydromica impurities, III, mostly chlorite rocks with a hydromica impurity, IV, chlorite–hydromica rocks, V, chlorite–smectite–hydromica rocks, VI, hydromica rocks with a significant impurity of dispersed feldspar.

In the FI-NAI diagram of clay rocks (Fig. 3), the composition points of the deposits form clusters.

Most of the points fall in field VI of hydromica rocks with a significant impurity of dispersed K-feldspars and in superposed field V of chlorite–smectite–hydromica rocks. Thus, the paleosols and substrate do not differ in clay mineral assemblages.

The index of compositional variability (ICV) of the deposits ranges from 0.8 to 1.3, which argues for a predominance of non-clay silicate minerals (the ICV values smaller than unity indicate a low degree of rock maturity, i.e., a small amount of clay minerals, in the sedimentation area).

The variations in the values of major lithochemical indicators of paleoclimate (CIA, CIW, and PIA) point to a predominance of arid and subarid depositional environments. The same follows from the location of the composition points of the section deposits in the Erofeev–Tsekhovskii diagram (Erofeev and Tsekhovskii, 1983) (Fig. 4). The maximum values of CIW and PIA are typical of the paleosol horizons (layers 1 and 14).

The variations in petrochemical indices and paleoclimate indicators throughout the section are shown in Fig. 5, and the variations in geochemical indices, in Fig. 6.

The values of the titanium index (TI) were used to identify the paleoclimate. The TI variations throughout the section (Fig. 5) indicate that the lower unit (Tologoi 1) accumulated in a warm arid climate; the middle unit (Tologoi 2), in

a colder and more humid climate; and the upper unit (Tologoi 3), in a more arid climate with the accumulation of precipitation.

The TI variations are consistent with the changes in the grain size composition of rocks and in the CIA and ICV values (Fig. 5).

The CIA values of the deposits vary from 49 to 69, averaging 65, which confirms the insignificant alteration of rocks in the catchment paleoareas. The CIA and ICV variations are synchronous; the CIA increase and simultaneous ICV decrease mark the humid-climate periods.

The AI values (Fig. 4) indicating the content of clay minerals vary from 0.19 to 0.25, which means an insignificant fractionation of the material during its transfer and its weak transformation during weathering.

The distribution of petrochemical and geochemical indices throughout the section shows weak geochemical stratification. There are no differences between the paleosols and the host loess-like sandy loams and loams: They contain similar clay mineral assemblages. This might be the result of fluvial processes and the postsedimentary transformation of the deposits under cryogenesis conditions.

The above transformation of sediments depends mostly on their initial composition (the presence of minerals and active components resistant to cryogenic weathering, such as colloidal forms of iron, aluminum, and manganese compounds, carbonates, soluble salts, etc.), the presence of organic matter, and the nature of the pore solution. Clay minerals are characterized by high dispersion, large specific surface area, hydrophilic properties, and capability for adsorption and ion exchange. It is obvious that the chemical composition of the clay fraction of the dispersed deposits generally reflects the degree of cryogenic alteration of the sediments.

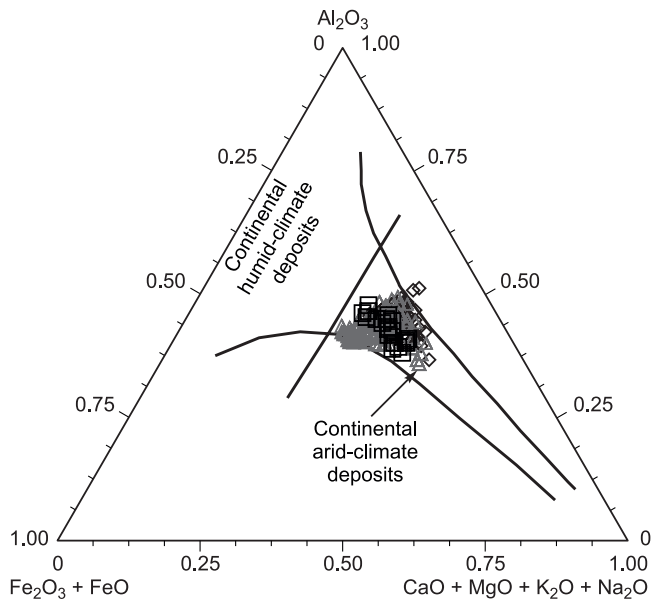


Fig. 4. Erofeev–Tsekhovskii diagram for the Tologoi units of different ages. Designations follow.

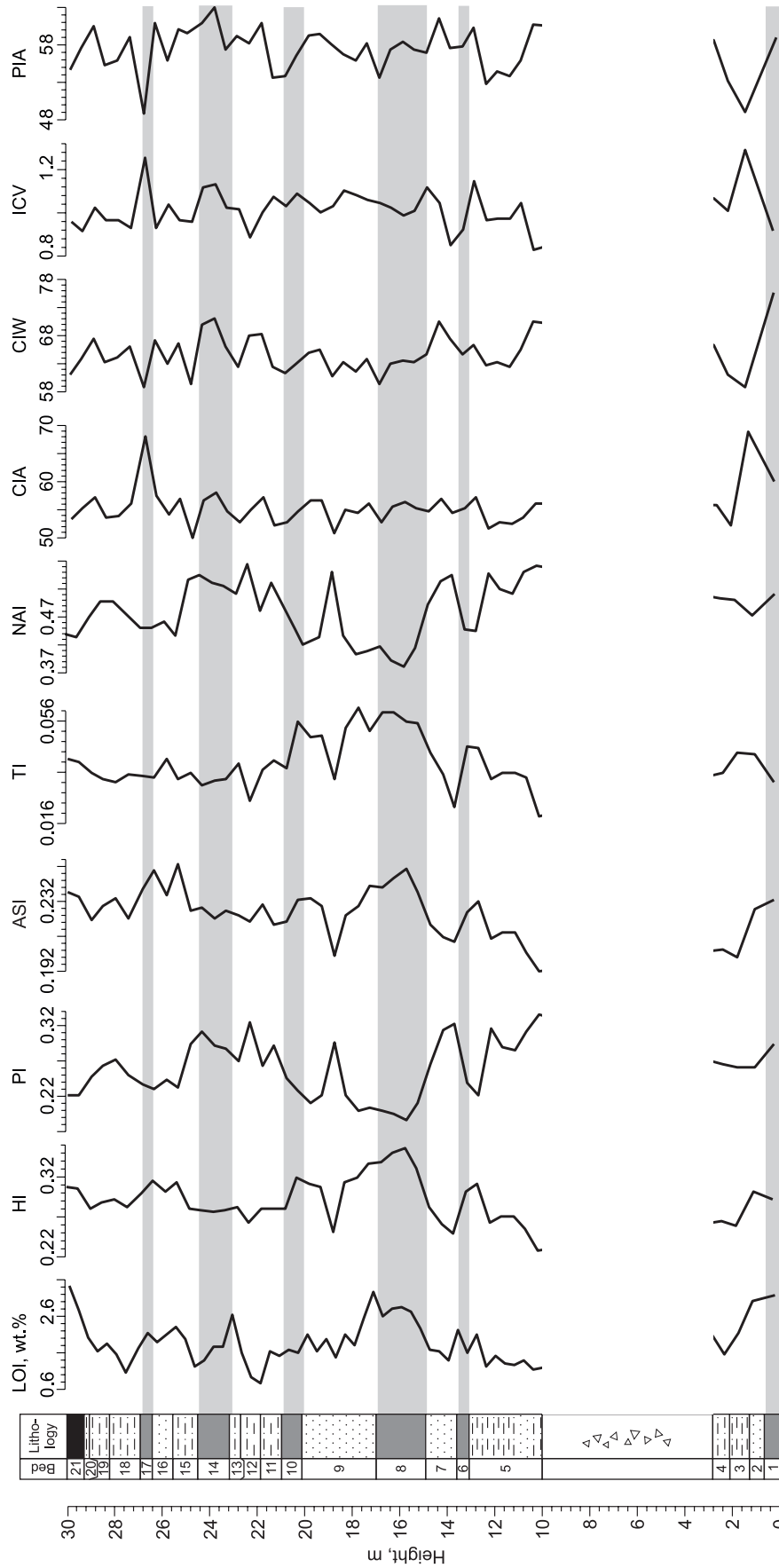


Fig. 5. Distribution of petrochemical indices and paleoclimate indicators in the geochemical profile. The legend to the lithologic column follows Fig. 1.

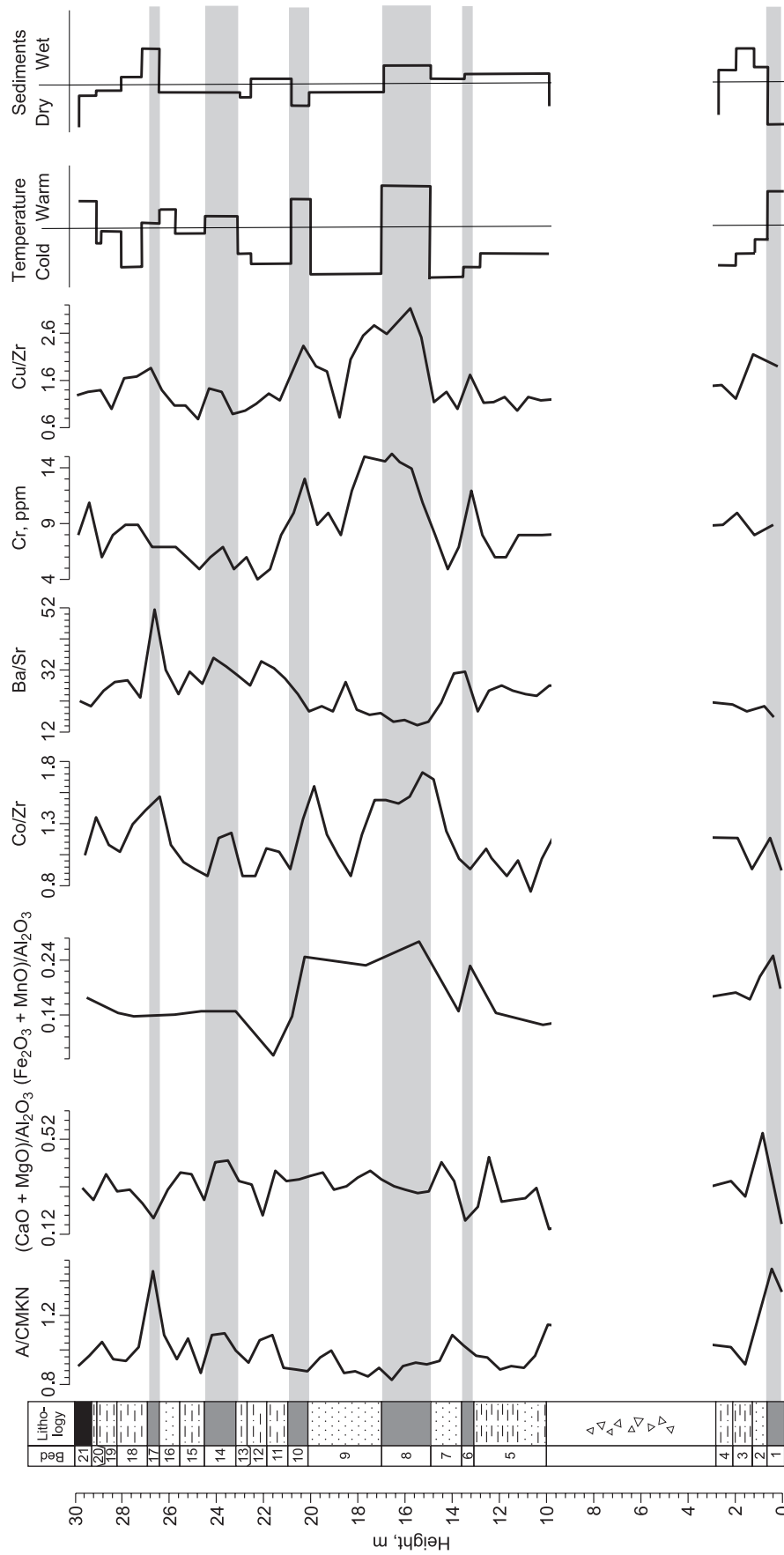


Fig. 6. Distribution of geochemical indices in the profile. Hypothetical temperature and humidity changes reconstructed on the basis of geochemical data for the depositional environment (on the right). The legend to the lithologic column follows Fig. 1.

Variations in the A/CMKN ($\text{Al}_2\text{O}_3/(\text{CaO} + \text{MgO} + \text{Na}_2\text{O} + \text{K}_2\text{O})$) values (Fig. 5) marking the quantitative ratio of relatively insoluble (clay) components to the components separated during hydrolysis (Grazhdankin and Maslov, 2012) show that most of the section (layers 5–16) formed during repeated cyclic freezing–thawing processes: The A/CMKN values smaller than unity and the simultaneous increase in the calcification index $(\text{CaO} + \text{MgO})/\text{Al}_2\text{O}_3$ of paleosols indicate authigenic formation of carbonates.

The paleosol horizon (layer 17) is characterized by high values of $\text{Al}_2\text{O}_3/(\text{CaO} + \text{MgO} + \text{Na}_2\text{O} + \text{K}_2\text{O})$ and $(\text{CaO} + \text{MgO})/\text{Al}_2\text{O}_3$. The variations in oxidation intensity, marked by the $(\text{Fe}_2\text{O}_3 + \text{MnO})/\text{Al}_2\text{O}_3$ ratio, are maximum for the paleosol of layer 1 (Tologoi 1) and paleosols of the middle section (Tologoi 2, layers 8 and 10).

The high Ba/Sr values point to hydrolysis.

The change in geochemical paleomarkers (Co/Zr, Cu/Zr, and Cr content) throughout the section (Fig. 6) permits a geochemical stratification of the section and leads us to the following conclusions:

- in general, the distribution of these paleomarkers reliably depicts the climate changes;
- in cold periods, when a seasonally thawed layer existed, Co and Cr were removed from the deposits more intensely as compared with permafrost-free strata, whereas Zr was inert; therefore, a decrease in the paleoparameter values marks a cold period, and vice versa;
- the most drastic climate variations are recorded in the middle section (horizons 10–20 m).

The data obtained show cyclic climate changes during the formation of the section deposits: The wet periods alternated with dry epochs of different durations. The position of the paleosol horizons is consistent with that established from the grain size parameters. The identified paleosol layer (the section interval 24.5–23.4 m) is clearly expressed in the geochemical profile.

The stage of accumulation of the paleosol horizon of layer 8 (the interval 16.4–15.0 m) was characterized by the warmest conditions and active weathering and leaching, which were accompanied by various soil processes and biologic activity and by the weakening of salinization and carbonation.

The geochemical data record a drastic deterioration of climatic conditions between the paleosol horizons in the section intervals 16.4–15.0 m and 13.6–13.0 m. The content of organic matter (LOI) decreases, the Cr content, Co/Zr, and Cu/Zr decrease, the values of all petrochemical indices also become smaller (the only exception is NAI, marking the ratio of readily soluble components to clay ones, which increases, because the amount of the clay fraction decreases, i.e., weathering becomes less intense). According to Alekseeva (2005), it is this section interval that involves a large pseudomorph after an ice wedge intruded into the underlying soil and ruptured. The same behavior of petro- and geochemical indices is recorded in the section interval 20.0–16.4 m.

Based on the geochemical data obtained, we have constructed a hypothetical model of the climate changes during

the formation of the Tologoi sedimentary section (Fig. 6, on the right). The examined geochemical profile clearly shows stages with dominating cryogenic environments in the study area: These are the periods of formation of layers 5, 7, 9, and 11–13. The deposits of these layers are characterized by the minimum salinization, high carbonation, and low leaching and oxidation indices.

REE signatures. The REE signatures of all samples of the Quaternary deposits are similar. They are characterized by excess of LREE and a relative deficit of HREE; $\text{LREE}/\text{HREE} = 1.7\text{--}2.4$. The REE tetrad effect calculated for the third (Nd, Sm, Eu, and Gd) and fourth (Er, Tm, Yb, and Lu) tetrads is close to the *M* type (its values vary from 0.9 to 1.1). The Tologoi section rocks differ little in ΣREE contents (Fig. 7), which indicates low sedimentation rates (Balashov, 1976).

The cerium anomaly is not pronounced; its average value is 0.96. Most samples show a Eu anomaly (1.10–1.23), which suggests the significant amounts of plagioclase in the section deposits.

The LREE, MREE, and HREE fractionation in the sediments is due to the different ratios of Fe and Mn oxides (hydroxides). Light REE are adsorbed on these mineral phases in larger amounts and faster than heavy REE, especially when the pH of the solution increases (De Baar et al., 1988). The data in Fig. 7 show that the paleosol horizons are maximally enriched in LREE.

The high $\Sigma\text{Ce}/\Sigma\text{Y}$ values (on average, 6.53) are due to the enrichment of the fine fraction of the deposits in feldspar and hydromica and to the transformation of hydromica during cryogenic weathering.

The main mechanisms responsible for the REE fractionation (selective REE enrichment as a result of the removal of various lanthanides from the sediments) are sorption, ion exchange reactions, reactions of isomorphous substitution of alkaline earth metals in the structure of rock-forming and authigenic minerals, and complexation (Ivanova et al., 2017). The degree of REE fractionation depends, first of all, on the acid–base conditions of the medium and on the ionic strength of the solution. In the case of early diagenesis of deposits under cryogenic conditions, an increase in the alkalinity of pore solutions and their high ionic strength will lead to the MREE enrichment of the clay fraction. Medium REE are adsorbed on clay particles or enter into ion exchange reactions with cations of alkali and alkaline earth metals in the hexagonal interlayer holes in the clay mineral structure. Light REE are adsorbed predominantly on iron and manganese hydroxo compounds and also participate in the isomorphous substitution of Ca^{2+} in the structure of authigenic or rock-forming minerals. When sorption processes dominate, the La/Yb ratio increases, while the La/Sm ratio does not change. When isomorphous substitution dominates, the La/Sm ratio increases, while in the case of chemisorption it decreases; the La/Yb ratio changes insignificantly.

The $(\text{La}/\text{Yb})_N - (\text{La}/\text{Sm})_N$ correlation established for the section rocks (Fig. 7) reflects the type of REE fractionation

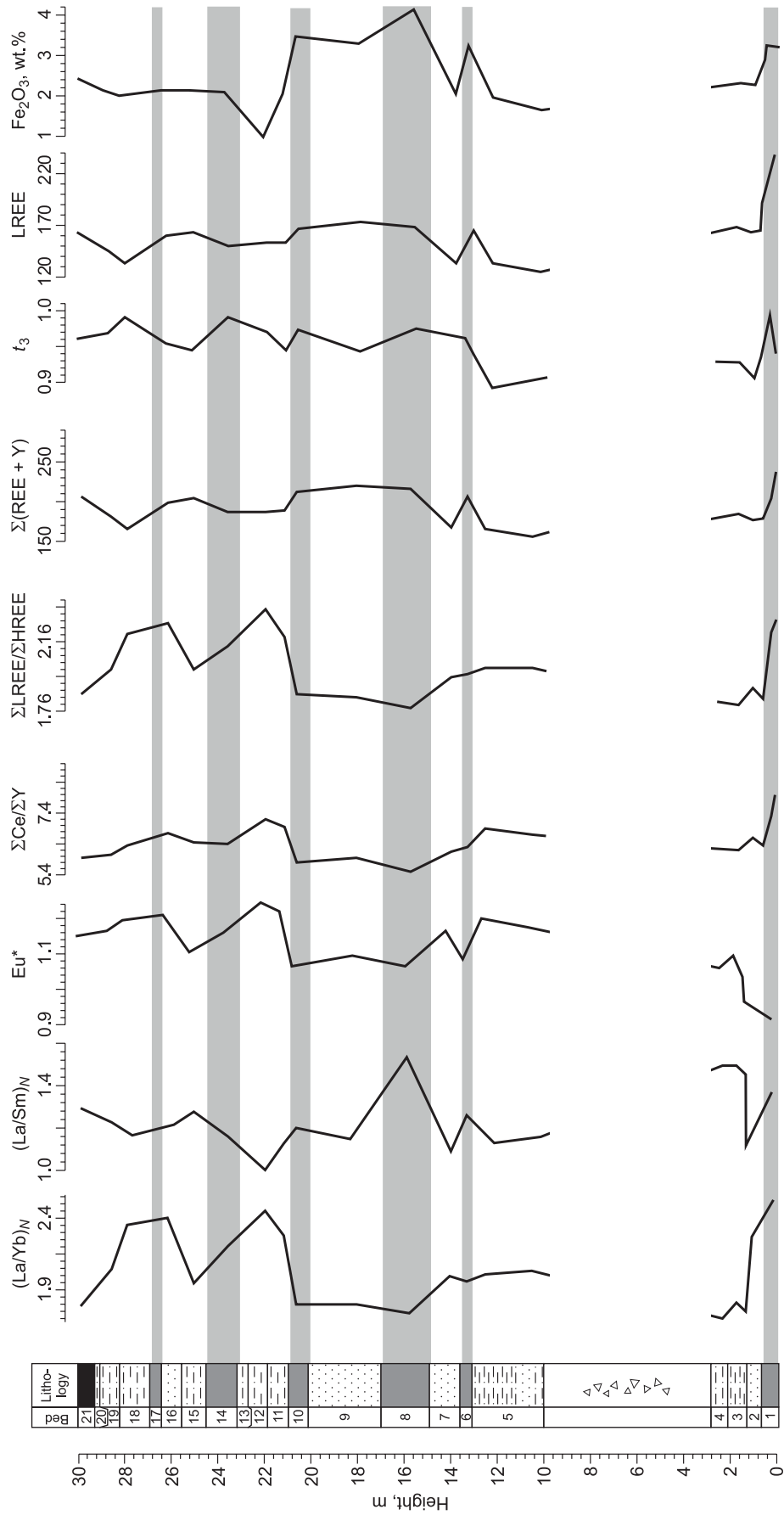


Fig. 7. Variations in the REE fractionation indices in the geochemical profile. The legend to the lithologic follows on Fig. 1.

in the aqueous medium (pore solutions) and sediments. The La/Yb ratio is within 1.70–2.54 (the median value is equal to 2), and La/Sm is within 1.03–1.57 (the median value is equal to 1.15).

It is obvious that both sorption and isomorphous substitution played a leading role in the REE fractionation. This is confirmed by the nearly *M*-type tetrad effect of the third and fourth REE tetrads. Usually, the *M*-type tetrad effect points to the association of REE with the solid phase (Masuda et al., 1987).

The distribution of the $(La/Yb)_N$ and $(La/Sm)_N$ values throughout the section makes it possible to distinguish zones with cryogenesis, namely, layers 5, 7, 9, and 11–13.

In some samples (Fig. 7), REE of the third tetrad (t_3) show a nearly *M*-type tetrad effect close to the threshold of statistical significance. Its maximum changes are observed mainly in the paleosol horizons. The weaker tetrad effect in some horizons might indicate cryogenic conditions, because it reflects MREE fractionation.

CONCLUSIONS

The revision of the Tologoi section made it possible to identify the following specifics of sedimentation and the early diagenesis of the deposits:

(1) Cyclic sedimentation traced from the behavior of all grain size fractions and, especially, from the change in sand content. Four main sedimentation cycles have been identified within the Tologoi 2 and Tologoi 3 units; each of them terminated with the formation of soil horizons (pedocomplexes).

(2) Sedimentary material was transported to the sedimentation site mainly from a proximal source. During warming and the formation of soil horizons, wind gusts and strength were reduced, and distant and medium-range provenance areas prevailed. In the periods of the most intense pedogenesis, the supply of sandy material decreased, sometimes to zero (Fig. 2), and *in situ* biochemical postsedimentary transformations of the deposits dominated.

(3) If the specific grain size parameters of the deposits were climate-controlled, then we assume that this area of the Selenga River valley had an arid climate with a minor humidity increase in the periods of pedogenesis. In dry periods, strong hurricane gusts and intense eolian processes were likely.

(4) The deposits of the Tologoi 2 unit (the section interval 20–10 m) formed in quieter wind conditions as compared with the Tologoi 3 unit.

(5) The grain size composition of the deposits reflects the specific sedimentation, pedogenesis with cryogenic transformation of the substrate, and deluvial redistribution of material along the slope. Taking into account the grain size composition, we interpret the genesis of the Tologoi 2 and Tologoi 3 deposits as deluvial (or eolian–deluvial and secondary deluvial).

(6) There were cyclic climate changes during the formation of the section deposits: The wet periods alternated with dry epochs of different durations.

(7) The stage of accumulation of the paleosol horizon of layer 8 (interval 16.4–15.0 m) was characterized by the warmest conditions and active weathering and leaching, which were accompanied by various soil processes and biologic activity and by the weakening of salinization and carbonation.

(8) The examined geochemical profile clearly shows stages with dominating cryogenic environments in the study area: These are the periods of formation of layers 5, 7, 9, and 11–13. The deposits of these layers are characterized by the minimum salinization, high carbonation, and low leaching and oxidation indices, a positive Eu anomaly, and high $\Sigma Ce/\Sigma Y$ and low $(La/Sm)_N$ values.

(9) The distribution of petrochemical and geochemical indices throughout the section shows weak geochemical stratification. There are no differences between the paleosols and the host loess-like sandy loams and loams: They contain similar clay mineral assemblages. This might be the result of fluvial processes and the postsedimentary transformation of the deposits under cryogenesis conditions.

This work was financially supported by grant 19-17-00216 (geochemistry and granulometry) from the Russian Science Foundation, grants 15-05-01858, 16-05-00586, 18-05-00215, and 20-05-00247 from the Russian Foundation for Basic Research, integration project 0341-2016-001, and project 075-15-2019-866.

REFERENCES

- Akul'shina, E.P., 1990. Riphean and Phanerozoic evolution of the physicochemical conditions of sedimentation (by the example of Siberia), in: Environment and Life in the Geologic Past [in Russian]. Nauka, Novosibirsk, pp. 17–26.
- Aleksandrova, L.P., Vangengeim, E.A., Gerbova, V.G., Golubeva, L.V., Ravskii, E.I., 1963. New data on the Anthropogene sedimentary section of Mt. Tologoi (western Transbaikalia). Byulleten' Komissii po Izucheniyu Chetvertichnogo Perioda, No. 28, 84–101.
- Alekseeva, N.V., 1994. New data on the time of permafrost formation in Transbaikalia, in: Abstracts of the International Meeting "Baikal, a Natural Laboratory for Studying Environmental and Climate Changes" [in Russian]. Lisna, Irkutsk, Vol. 2, pp. 1–2.
- Alekseeva, N.V., 2005. Late Cenozoic Evolution of the West Transbaikalian Environment (according to Data on Small Mammals) [in Russian]. GEOS, Moscow.
- Alexeeva, N.V., Erbajeva, M.A., 2000. Pleistocene permafrost in Western Transbaikalia. Quat. Int. 68–71, 5–12.
- Andreeva, D.B., Leiber, K., Glaser, B., Hambach, U., Erbajeva, M., Chimitdorzhieva, G.D., Tashak, V., Zech, W., 2011. Genesis and properties of black soils in Buryatia, southern Siberia, Russia. Quat. Int. 243, 313–326.
- Balashov, Yu.A., 1976. Geochemistry of Rare-Earth Elements [in Russian]. Nauka, Moscow.
- Balashov, Yu.A., 1985. Isotope-Geochemical Evolution of the Earth's Mantle and Crust [in Russian]. Nauka, Moscow.
- Bazarov, D.B., 1968. Quaternary Deposits and Major Stages of Evolution of the Selenga Midland Relief [in Russian]. Buryatskoe Knizhnoe Izd., Ulan-Ude.

- Bazarov, D.B., 1986. The Cenozoic of Cisbaikalia and Western Transbaikalia [in Russian]. Nauka, Novosibirsk.
- Berezin, P.N., 1983. Distribution of the grain size parameters of soils and soil-forming rocks. *Pochvovedenie*, No. 2, 64–72.
- Bibikova, V.I., Vereshchagin, N.K., Garutt, V.E., Yur'ev, K.B., 1953. New materials on the Quaternary fauna of Transbaikalia (Oshurkovo, Tologoi), in: *Archeology Materials and Research* [in Russian]. Moscow, Leningrad, Izd. AN SSSR, Issue 39, pp. 463–475.
- Blott, S.J., Pye, K., 2001. GRADISTAT: a grain size distribution and statistics package for the analysis of unconsolidated sediments. *Earth Surf. Processes Landforms* 26, 1237–1248.
- Cox, R., Lowe, D.R., Cullers, R.L., 1995. The influence of sediment recycling and basement composition on evolution of mudrock chemistry in the southwestern United States. *Geochim. Cosmochim. Acta* 59, 2919–2940.
- De Baar, H.J.W., German, C.R., Elderfield, H., van Gaans, P., 1988. Rare earth element distributions in anoxic waters of the Cariaco Trench. *Geochim. Cosmochim. Acta* 52, 1203–1219.
- Dobrovolskii, V.V., 1976. The Geography of Soils and the Basis of Soil Sciences [in Russian]. Prosveshchenie, Moscow.
- Elderfield, H., Greaves, M.J., 1982. The rare earth elements in seawater. *Nature* 296, 214–219.
- Erbaeva, M.A., 1970. The History of the Anthropogene Hares and Rodents of the Selenga Midland [in Russian]. Nauka, Moscow.
- Erofeev, V.S., Tschikovskii, Yu.G., 1983. Parageneses of Continental Deposits (Family of Arid Parageneses. Evolutionary Periodicity) [in Russian]. Nauka, Moscow.
- Fedo, C.M., Nesbitt, H.W., Young, G.M., 1995. Unraveling the effects of potassium metasomatism in sedimentary rocks and paleosols, with implications for paleoweathering conditions and provenance. *Geology* 23, 921–924.
- Folk, R.L., Ward, W.C., 1957. Brazos River bar: a study in the significance of grain size parameters. *J. Sediment. Petrol.* 27, 3–26.
- Gnibidenko, Z.N., Erbaeva, M.A., Pospelova, G.A., 1976. Paleomagnetism and biostratigraphy of some upper Cenozoic deposits of western Transbaikalia, in: *Mesozoic and Cenozoic Paleomagnetism of Siberia and the Far East* [in Russian]. IGiG SO AN SSSR, Novosibirsk, pp. 75–95.
- Gradziński, R., Kostecka, A., Radomski, A., Unrug, R., 1976. *Sedymetologia*. Wydawnictwa Geologiczne, Warszawa.
- Grazhdankin, D.V., Maslov, A.V., 2012. Lithochemistry of primitive paleosols in the middle section of the Bederysh Subformation of the upper Riphean Zil'merdak Formation at the southern edge of the town of Min'yar, in: *Yearbook 2011* (Transactions of the Institute of Geology and Geochemistry, UB RAS, Issue 159), pp. 77–84.
- Gromet, L.P., Haskin, L.A., Korotev, R.L., Dymek, R.F., 1984. The “North American shale composite”: Its compilation, major and trace element characteristics. *Geochim. Cosmochim. Acta* 48, 2469–2482.
- Irber, W., 1999. The lanthanide tetrad effect and its correlation with K/Rb, Eu/Eu*, Sr/Eu, Y/Ho, and Zr/Hf of evolving peraluminous granite suites. *Geochim. Cosmochim. Acta* 63, 489–508.
- Ivan'ev, L.N., 1966. Stratigraphic subdivision of Cenozoic red-colored deposits in western Transbaikalia according to paleontological data. *Izvestiya Vostochno-Sibirskogo Otdeleniya Geograficheskogo Obshchestva SSSR* 65, 88–94.
- Ivanova, V.V., 2012. Rare earth elements in the Pleistocene deposits of central and eastern Yakutia, in: *Proceedings of the Joint International Conference “Geomorphology and Paleogeography of Polar Regions”* [in Russian]. SPbGU, St. Petersburg, pp. 199–203.
- Ivanova, V.V., Shchetnikov, A.A., Filinov, I.A., Veshcheva, S.V., Kazansky, A.Yu., Matasova G.G., 2016. Litho geochemistry of rocks of the upper Neopleistocene Ust-Oda reference section in the Irkutsk amphitheater of the Siberian Platform. *Lithol. Mineral Resour.* 51 (3), 179–194.
- Ivanova, V.V., Nikolskiy, P.A., Basilyan, A.E., 2017. Stratigraphic interpretation of rare earth element signatures in Pleistocene mammal bones: A case study from Kharabai site, East Siberia. *Quat. Int.* 445, 279–288.
- Kalinin, P.I., Alekseev, A.O., Savko, A.D., 2009. Forests, Paleosols, and Paleogeography of the Quaternary Deposits of the Southeastern Russian Plain (Transactions of the Institute of Geology of Voronezh State University) [in Russian]. VGU, Voronezh, Issue 58.
- Kazansky, A.Yu., Matasova, G.G., Shchetnikov, A.A., Filinov, A.I., Erbaeva, M.A., 2018. Petromagnetic and grain size characteristics of the Quaternary deposits of the Tologoi reference section (Buryatia, Russia), in: *Geospace Problems. Proceedings of the 12th International School-Conference*, St. Petersburg, Peterhof, October 8–12, 2018 [in Russian]. OOO “Izdatel'stvo VVM”, St. Petersburg, pp. 105–112.
- Kučera, J., Cempírek, J., Dolníček, Z., Muchez, P., Prochaska, W., 2009. Rare earth elements and yttrium geochemistry of dolomite from post-Variscan vein-type mineralization of the Nížký Jeseník and Upper Silesian Basins, Czech Republic. *J. Geochem. Explor.* 103 (2–3), 69–79.
- Liskun, I.G., Rengarten, N.V., 1963. Composition and conditions of formation of the Anthropogene deposits of Mt. Tologoi (western Transbaikalia). *Bulletin of the Commission on the Study of the Quaternary Period*, No. 28, 101–110.
- Maslov, A.V., 2005. *Sedimentary Rocks: Methods of Study and Interpretation of the Obtained Data* [in Russian]. UGGU, Yekaterinburg.
- Maslov, A.V., 2006. Using litho- and geochemical data for the reconstruction of sedimentation conditions, in: *Metallogeny of Ancient and Recent Oceans. Proceedings of the 12th School-Conference* [in Russian]. IMin UrO RAN, Miass, pp. 25–30.
- Maslov, A.V., Krupenin, M.T., Petrov, G.A., Ronkin, Yu.L., Lepikhina, O.P., Kornilova, A.Yu., 2007. Certain geochemical features and conditions of sedimentation of fine-grained terrigenous rocks of Serebryanka and Sylvitsa groups (Middle Urals). *Litosfera*, No. 2, 3–28.
- Masuda, A., Kawakami, O., Dohmoto, Y., Takenaka, T., 1987. Lanthanide tetrad effects in nature: two mutually opposite types, W and M. *Geochem. J.* 21, 119–124.
- Monecke, T., Kempe, U., Monecke, J., 2002. Tetrad effect in rare earth element distribution patterns: A method of quantification with application to rock and mineral samples from granite-related rare metal deposits. *Geochim. Cosmochim. Acta* 66, 1185–1196.
- Nesbitt, H.W., Young, G.M., 1982. Early Proterozoic climates and plate motions inferred from major element chemistry of lutites. *Nature* 299, 715–717.
- Raukas, A.V., 1981. *Bottom Sediments of Lake Peipsi-Pihkva* [in Russian]. Izd. AN ESSR, Tallin.
- Ravskii, E.I., 1972. *The Anthropogene Sedimentation and Climates in Inner Asia* [in Russian]. Nauka, Moscow.
- Ravskii, E.I., Aleksandrova, L.P., Vangengeim, E.A., Gerbova, V.G., Golubeva, L.V., 1964. *Anthropogene Deposits of Southern East Siberia* [in Russian]. Moscow, Nauka.
- Retallack, G.J., 2001. *Soils of the Past: an Introduction to Paleopedology*. Blackwell, Oxford.
- Retallack, G.J., 2007. Soils and global change in the carbon cycle over geological time, in: *Holland, H.D., Turekian, K.K. (Eds.), Treatise on Geochemistry*. Pergamon Press, Oxford, Vol. 5, pp. 1–28.
- Reynard, B., Lécuyer, C., Grandjean, P., 1999. Crystal-chemical controls on rare-earth element concentrations in fossil biogenic apatites and implications for paleoenvironmental reconstructions. *Chem. Geol.* 155, 233–241.
- Ryashchenko, T.G., Akulova, V.V., Erbaeva, M.A., 2012. Formation of loess-like deposits in Transbaikalia (a case study on sample plots). *Geogr. Nat. Resour.* 4, 117–125.
- Shatrov, V.A., 2007. *Lanthanides as Indicators of Depositional Environments (Based on Analysis of the Proterozoic and Phanerozoic Key Sections of the East European Platform)*. ScD Thesis [in Russian]. Moscow.

- Taylor, S.R., McLennan, S.M., 1985. *The Continental Crust: Its Composition and Evolution*. Blackwell, Oxford.
- Trueman, C.N., Behrensmeyer, A.K., Potts, R., Tuross, N., 2006. High-resolution records of location and stratigraphic provenance from the rare earth element composition of fossil bones. *Geochim. Cosmochim. Acta* 70, 4343–4355.
- Vangengeim, E.A., 1977. Paleontological Substantiation of the Anthropogene Stratigraphy of North Asia [in Russian]. Nauka, Moscow.
- Vangengeim, E.A., Belyaeva, E.I., Garutt, V.E., Dmitrieva, E.L., Zazhigin, V.S., 1966. Eopleistocene Mammals of Western Transbaikalia [in Russian]. Nauka, Moscow.
- Vogt, T., Erbajeva, M., Vogt, H., 1995. Premières preuves de conditions périglaciaires au Pléistocène inférieur en Transbaikalie (Sibérie, Russie). *Comptes Rendus de l'Académie des Sciences de Paris, Série A* 320, 861–866.
- Yudovich, Ya.E., Ketris, M.P., 2000. *Principles of Lithochemistry* [in Russian]. Nauka, St. Petersburg.
- Zech, W., Andreeva, D., Zech, M., Bliedtner, M., Glaser, B., Hambach, U., Erbajeva, M., Zech, R., 2017. The Tologoi Record: a terrestrial key profile for the reconstruction of Quaternary environmental changes in semiarid Southern Siberia, in: *The 3rd Asian Association for Quaternary Research. Conference Abstract Book*. 4–8 September 2017, Jeju Island, Republic of Korea. Lotte City, p. 13.

Editorial responsibility: I.S. Novikov